EFFECT OF THE DOWNWASH FLOW FIELD OF A SINGLE-ROTOR UAV ON DROPLET VELOCITY IN SUGARCANE PLANT PROTECTION

Ping Zhang[1,3], Wei Zhang[1*], Haitian Sun[2], Haiba Fu[1], Jiansheng Liu[3,4]

[1*]Corresponding author. Heilongjiang Bayi Agricultural University/ Daqing, China.
E-mail: zhang66wei@126.com | ORCID ID: https://orcid.org/0000-0001-7921-2476

ABSTRACT

Protecting against the main sugarcane diseases and insect pests requires good control at the base of the plant; therefore, higher droplet penetration is required during plant protection. The objectives of this research were to explore the movement mechanism of droplets in a sugarcane protection operation using a single-rotor unmanned aerial vehicle (UAV) and establish the connection between the UAV downwash flow field and droplet penetration. By considering the downwash flow field of a single-rotor UAV in layers, a theoretical model of the vertical velocities of droplets was established, and verification experiments were carried out in a sugarcane field. The results showed that the velocity of the UAV downwash flow was the main factor affecting the final vertical velocity of the droplets, the final vertical velocity of a droplet was positively correlated with the droplet diameter, and the initial droplet velocity had no significant effect on the final droplet velocity. In the transportation of droplets, the droplet velocity quickly approached the velocity of the airflow, and the smaller the droplet diameter was, the higher the acceleration. These research results can provide guidance for the theoretical study of droplet deposition effects in sugarcane protection operations using single-rotor UAVs.

INTRODUCTION

Sugarcane is the most important sugar crop in the world, and the annual output of sucrose accounts for more than 76% of the total sugar produced (Canata et al., 2019; Feng et al., 2019; Zhou et al., 2016). Sugarcane is the most promising energy crop, accounting for 63.8% of ethanol fuel raw materials (Li & Yang, 2009; Stevanato et al., 2019). With the large-scale planting of high-yielding and high-sucrose varieties, sugarcane diseases and insect pests are increasingly common. Survey results show that the average yield loss rate of sugarcane harmed by cotton aphids and borers is 12%-16% and reaches 40%-60% in severe cases, and the sugar reduction rate can reach 0.93%-3.5% (Santos, 2019; Pan et al., 2009; Zhang et al., 2019).

Protecting against the main sugarcane diseases, such as sugarcane brown spot disease, and insect pests, such as sugarcane aphids and borers, mostly requires good control at the base of the plant; therefore, higher droplet penetration is required during spraying. The airflow of an unmanned aerial vehicle (UAV) can improve droplet penetration during spraying (He, 2004), and UAV plant protection operations are highly efficient, are not restricted by crop growth, can deal with explosive diseases and insect pests and can avoid problems that arise in the operation of ground machinery in the middle and later stages of crop growth. Although runoff can occur, the pesticide application rate is 20-30% lower than that of ground machines, and the pesticide cost is lower (Qin et al., 2016). The operation parameters of UAVs, such as flying height, operational speed and nozzle flow, have a considerable influence on penetration (Chen et al., 2017a). The airflow distributions in different directions of the wind field are closely related to the UAV flying height, flight speed and other operating parameters. When the flying height increases, the vertical velocity of the UAV downwash flow near the crop canopy

will decrease (An et al., 2013; David et al., 2014; Lee et al., 2014; Zhu et al., 2013). The downwash airflow of UAVs is the direct cause of the change in droplet penetration, and vertical wind speed has a greater effect than horizontal wind speed. Droplet penetration is positively correlated with the vertical velocity of airflow (Chen et al., 2017b).

The above studies indicate that the relationship between UAV operation parameters and downwash flow distribution has been researched, and the influence of downwash flow on droplet penetration has also been studied. However, the relationship between wind field velocity and droplet velocity has not been reported, which makes the influence of UAV downwash flow on droplet penetration lack theoretical support.

In this paper, based on analyzing the specific distribution of the downwash flow field of a single-rotor UAV, the movement of droplets in the flow field was theoretically studied, and the relationship between the downwash flow velocity and the droplet velocity was quantitatively described. This study aims to provide theoretical guidance for establishing a deposition parameter model such as a droplet penetration model.

MATERIAL AND METHODS

Theoretical analysis

Droplet kinetic equation and solution method

To study the motion of droplets in the downwash flow field of a single-rotor UAV and reveal the influence of airflow on droplet velocity, it is necessary to analyze the forces on the droplets, establish a kinetic equation, and then identify the relationship between the parameters to be solved and the initial variables.

When droplets are transported, they are mainly subject to the combined effects of gravity $\vec{F}_g$ and air drag force $\vec{F}_D$ (Fritz et al., 2009). According to Newton's second law, the kinetic equation of a droplet is

$$m_p \frac{d\vec{v}_p}{dt} = \vec{F}_g + \vec{F}_D \tag{1}$$

$\vec{v}_p$ is the droplet velocity, and gravity takes the following form:

$$\vec{F}_g = \frac{1}{6}\pi d_p^3 \rho_p \tag{2}$$

d_p is the droplet diameter, and ρ_p is the droplet density. The air drag force is expressed as

$$\vec{F}_D = \frac{1}{8}\pi C_d d_p^2 \rho_f |\vec{v}_f - \vec{v}_p|(\vec{v}_f - \vec{v}_p) \tag{3}$$

Where:

ρ_f is the air density;

$\vec{v}_f$ is the airflow velocity, and

C_d is the drag coefficient, which takes the following form:

$$C_d = C_{D0} \frac{2\mu_g + 3\mu_d + k}{3\mu_g + 3\mu_d + k} h \tag{4}$$

The aerodynamic viscosity is $\mu_g = 1.8 \times 10^{-5} N \cdot s \cdot m^{-2}$, the hydrodynamic viscosity is $\mu_d = 0.001 N \cdot s \cdot m^{-2}$, k is the flow rate of the inner ring of the droplet because inner ring flow is ignored, and $k = 0$. The amount of liquid deformation is $h = 1$, and $C_d = 0.994 C_{D0}$, where

$$C_{D0} = \begin{cases} 24/Re, Re < 6.2, \\ 10Re^{-1/2}, 6.2 \leq Re < 500, \\ \frac{24}{Re}(1 + 0.15Re^{0.687}), 500 \leq Re < 800, \\ 0.44, 800 \leq Re < 2 \times 10^5, \end{cases} \tag{5}$$

R_e is the Reynolds number and expressed as

$$R_e = \frac{d|\vec{v}_f - \vec{v}_p|\rho_f}{\mu_g} \tag{6}$$

Substituting eqs (2) and (3) into [eq. (1)] gives

$$m_p \frac{d\vec{v}_p}{dt} = \frac{1}{8}\pi C_d d_p^2 \rho_f |\vec{v}_f - \vec{v}_p|(\vec{v}_f - \vec{v}_p) - \frac{1}{6}\pi d_p^3 \rho_p g \tag{7}$$

By integrating [eq. (7)], the output parameters, such as the velocity and displacement, can be obtained.

Because C_d is a function of R_e and R_e is a function of v_p, it is difficult to obtain the analytic solution to [eq. (7)]. These complex equations can be solved by using a numerical method (Ahmed & Youssef, 2014; Yang et al., 2013); thus this model uses the fourth-order Runge-Kutta method to calculate the droplet velocity, and then, the variation in droplet velocity can be obtained. Since the horizontal velocity has very little influence on droplet penetration, this paper studies only the change rules in the vertical droplet velocities. When up is taken to be the positive direction of the Y-axis, the vertical acceleration of the droplet can be expressed as

$$a_y = \frac{1}{8m_p}\pi C_d d_p^2 \rho_f |\vec{v}_{fy} - \vec{v}_{py}|(\vec{v}_{fy} - \vec{v}_{py}) - g \tag{8}$$

According to the vertical acceleration a_y and the initial vertical velocity v_{y0}, the velocity v_y can be obtained by using the fourth-order Runge-Kutta method as follows:

$$\begin{cases} k_1 = a_{y(n)} \\ k_2 = a_{y(n)} + \frac{t}{2} * k_1 \\ k_3 = a_{y(n)} + \frac{t}{2} * k_2 \\ k_4 = a_{y(n)} + t * k_3 \\ v_{y(n+1)} = v_{y(n)} + \frac{t}{6} * (k_1 + 2k_2 + 2k_3 + k_4) \end{cases} \tag{9}$$

In addition to the velocity of the UAV downwash flow field, the parameters that may affect the final vertical droplet velocity include the initial vertical velocity and the droplet diameter. To explore the relationship between the final vertical and initial vertical velocities and the droplet diameter, it is necessary to determine the value range of each parameter in the calculation process. The maximum initial velocity of the droplet for centrifugal nozzles is approximately 15 m/s (Zhou et al., 2017), and it is approximately 19 m/s for hydraulic nozzles (Song et al. 2007). The range of initial vertical velocities was set as 0-15 m/s in our study, with an interval of 3 m/s. The droplet diameter range of diseases and insect pest controls should be 30-150 μm (Yuan & Wang, 2015). As the actual range of droplet sizes is often slightly greater, the range of droplet diameters was set as 30-210 μm, with an interval of 30 μm.

Downwash flow field of a UAV

A TY-800 single-rotor UAV provided by Eagle Brother Co., Ltd., in Shenzhen, China (Figure 1), with a fully automatic flight control system, was selected for the experiments. Its specific parameters are shown in Table 1. The boom length is 1.5 m, with one nozzle on each end.

FIGURE 1. TY-800 single-rotor UAV.

TABLE 1. Parameters of the TY-800 single-rotor UAV

Parameters	Value
Gross mass (kg)	54
Diameter of the main rotor (mm)	2455
Tank volume (L)	25
Length of the lance boom (mm)	1345
Motor power (kW)	8

The vertical velocity of the downwash flow of a single-rotor UAV has a significant influence on droplet penetration (Chen et al., 2017d). The distribution of the downwash flow field of the TY-800 single-rotor UAV was simulated (Figure 2) with the method described in the research of Yang et al. (2018).
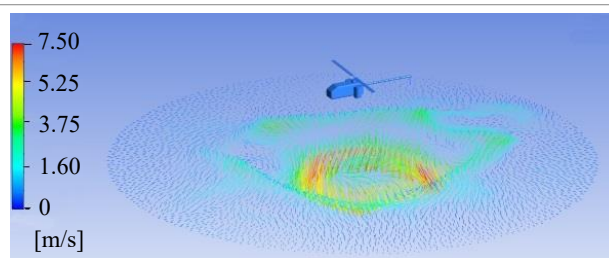

FIGURE 2. Downwash flow field of the TY-800 single-rotor UAV

To ensure that the airflow and droplets penetrate the canopy, the airflow should meet the final velocity principle (Wei et al., 2016). That is, the airflow near the crop canopy must have a certain speed. According to the characteristics of the crop canopy morphology structure, the final velocities are generally 2-4 m/s. The nozzle was located 0.5 m below the plane of the rotor. The vertical velocity of the downwash flow was approximately 7.5 m/s near the nozzle and 1.8 m/s 3.0 m below the nozzle. To meet the final velocity principle, the height difference between the UAV and crop canopy was set to 3.5 m. To quantitatively describe the influence of the downwash flow of the UAV on the droplet velocity and analyze the change rules in the droplet velocity, the downwash flow field of the UAV was simplified: uniform flow field layers were set every 0.5 m in the vertical direction, and the flow speed of each layer was calculated by averaging the actual speed data (Table 2).

TABLE 2. Vertical velocity distribution.

	Distance below the nozzle plane (m)					
	0-0.5	0.5-1.0	1.0-1.5	1.5-2.0	2.0-2.5	2.5-3.0
Velocity (m/s)	7.5	5.2	3.8	3.5	2.8	1.8

Material and verification experiment methods

Experimental conditions

To study the effect of the downwash flow field of the UAV and initial droplet vertical velocity on droplet penetration, spray experiments were carried out with the single-rotor UAV in a sugarcane field of the Tropical Agricultural Machinery Research Institute in Zhanjiang (110°13'50.566"E, 21°12'36.882"N), Guangdong Province, China. The experiment was conducted on December 10, 2019. The temperature was 25°C, and there was no wind during the experiment. The sugarcane field dimension was 50 m×50 m, the sugarcane height ranged from 3.0 to 3.5 m, and the planting density was approximately 48000 plants/ha.

Experimental design

As the pretest showed that the effective spray width of droplets was within 8 m, two rows of sampling rods were arranged in the sugarcane field, with 17 rods in each row and a rod spacing of 0.5 m (Figure 3). There were two layers of fixed water-sensitive paper on each rod, and the heights of the upper and lower layers were 3.0 m and 1.5 m, respectively. The water-sensitive paper had the following dimensions: 0.03 m×0.02 m.
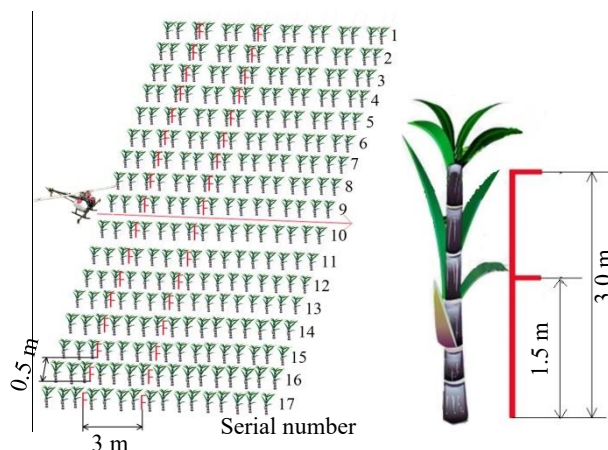

FIGURE 3. Arrangement of the sampling rods.

A Mayatech-12 centrifugal nozzle (Figure 4) with an atomizing disc with a 0.06 m outer diameter was selected for the experiments. The droplet spectrum was 50-200 μm (VMD), and the suitable spray volume was 0.1-1.5 L/min. The conical nozzle used in the experiment was a Teejet TX-VK6 nozzle, the suitable spray volume was 0.5-1.0 L/min, and the droplet spectrum was 50-160 μm (VMD).
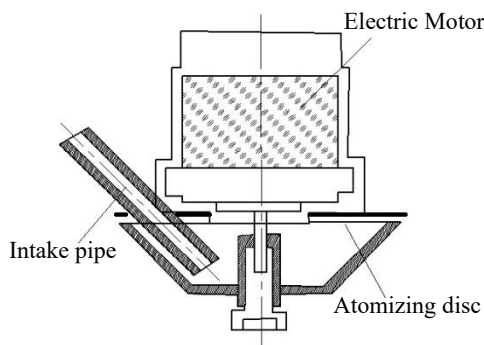

FIGURE 4. Mayatech-12 centrifugal nozzle.

The UAV flew uniformly along the centerline according to the preset operating parameters, and water was used instead of pesticide in the experiment. Each flight of the UAV started 20 m from the sampling area to ensure the high accuracy of droplet collection.

According to the research of Qin (2017) and the characteristics of the TY-800 UAV parameters, the operation parameters of the TY-800 single rotor UAV are shown in Table 3.

TABLE 3. Experimental parameters.

Treatment	Nozzle type	Flying height (m)	Flight velocity (m/s)
1	Centrifugal nozzle	5.5	2.5
2	Centrifugal nozzle	6.0	2.5
3	Centrifugal nozzle	6.5	2.5
4	Cone nozzle	6.0	2.5

To ensure that the droplets of the cone nozzle and the centrifugal nozzle had the same size, the nozzle operating parameters were controlled as presented in Table 4. The droplet size of the centrifugal nozzle was controlled by the rotating speed of the atomizing disc, and the droplet diameter of the cone nozzle was controlled by the flow rate of the water. The initial droplet velocity of the centrifugal nozzle was calculated based on the outside diameter and rotation speed of the atomizing disc (Zhou et al. 2017), and the initial droplet velocity of the cone nozzle was obtained by solving the Bernoulli equation and continuity equation (Song et al. 2007).

TABLE 4. Nozzle operating parameters.

Nozzle type	Spray volume (L/min)	VMD (μm)[a]	Initial vertical velocity (m/s)
Centrifugal nozzle	0.75	130-150	0
Cone nozzle	0.60	140-160	10-12

[a] VMD represents the volume median diameter of the droplets

The collected water-sensitive papers were scanned by an HP-200 scanner, and the scanned images were analyzed by Deposit Scan (V1.2). To improve the accuracy, the deposition amounts of the two rows of sampling rods were averaged.

RESULTS AND DISCUSSION

Theoretical studies

Results and regression analysis of vertical droplet velocity

According to Eq. (10), the final vertical velocities of the droplets in the layered flow field can be obtained (Table 5).

TABLE 5. Statistical table of the final droplet velocities.

Droplet diameter (μm)	Initial velocity (m/s)	Final vertical velocity (m/s)	Droplet diameter (μm)	Initial velocity (m/s)	Final vertical velocity (m/s)
30	0	1.92619	120	9	2.30664
30	3	1.92619	120	12	2.30653
30	6	1.92619	120	15	2.30654
30	9	1.92619	150	0	2.44006
30	12	1.92619	150	3	2.43963
30	15	1.92619	150	6	2.44006
60	0	2.05238	150	9	2.44006
60	3	2.05238	150	12	2.44006
60	6	2.05238	150	15	2.43963
60	9	2.05238	180	0	2.58330
60	12	2.05238	180	3	2.58437
60	15	2.05238	180	6	2.58330
90	0	2.17868	180	9	2.58330
90	3	2.17867	180	12	2.58231
90	6	2.17867	180	15	2.58331
90	9	2.17868	210	0	2.73783
90	12	2.17867	210	3	2.73783
90	15	2.17867	210	6	2.73963
120	0	2.30653	210	9	2.73786
120	3	2.30643	210	12	2.73777
120	6	2.30654	210	15	2.73968

The regression analysis results are presented in Table 6:

TABLE 6. Regression analysis results.

Parameters	Regression coefficient	P-value
Droplet diameter	0.00448	1.16971×10^{-56}
Initial velocity	8.70873×10^{-7}	0.99788
Constant term	1.78080	7.87298×10^{-30}

As the P-value of the initial droplet velocity is greater than 0.05, the initial velocity does not have a significant influence on the final velocity and should be removed. The P-value of the droplet diameter is less than 0.01, so it has a highly significant influence on the final velocity. According to Table 6, the linear regression equation is as follows:

$$V_y = 0.00448d + 1.78080 \qquad (10)$$

Where:

V_y is the droplet vertical velocity, and

d is the droplet diameter.

In the regression analysis model, $R^2 = 0.998$, the fitting degree is high, and the data points are concentrated near the regression line. The P-value of the significance coefficient of the equation is 4.48204×10^{-58}, which is less than 0.01; thus, the equation describes a significant linear relationship, and the model is reliable.

Change rules of vertical droplet velocity

According to [eq. (10)], it can be concluded that the final droplet velocity will increase with increasing droplet diameter, which is consistent with the research conclusions of Gao & Zhao (2020). However, due to the small coefficient of the droplet diameter, the final droplet velocity mainly depends on the constant term. Taking the 90 μm droplet as an example, the calculation result of the one-degree term of [eq. (10)] is 0.40320, far less than the constant term of 1.78080. The final velocity of the downwash flow of the UAV has a significant effect on the constant term and is the main factor that influences the final velocity of the droplet.

Under the action of downwash flow, the droplet velocity will quickly approach the downwash flow velocity. For the 90 μm droplet, the velocity variation process can be completed in approximately 0.03 s (Figure 5). The droplet acceleration will decrease when the droplet diameter increases and will increase with the increase of the difference between the downwash flow velocity and the droplet velocity (Figures 5 and 6). If the area of the uniform flow field is large enough, the droplet velocity will reach a certain critical value, and then, the droplet will move uniformly at this speed.
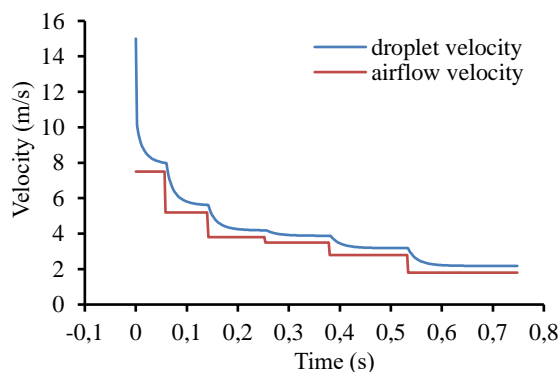

FIGURE 5. Comparison diagrams of the airflow velocity and the velocity of droplets with a diameter of 90 μm
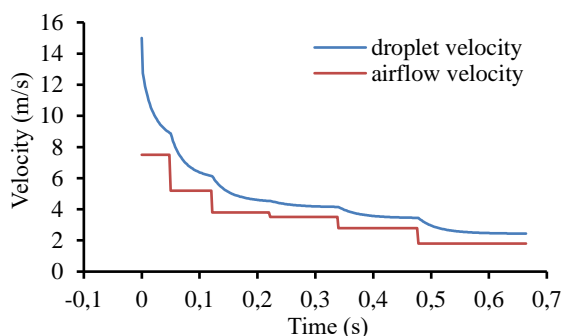
FIGURE 6. Comparison diagrams of the airflow velocity and the velocity of droplets with a diameter of 150 μm.

According to the above analysis, the velocity of droplets near the canopy mainly depends on the velocity of the downwash flow of the single-rotor UAV. Thus, when the vertical velocity of the downwash flow of the UAV increases, the final vertical velocity of droplets will also increase. According to the research conclusion of Chen et al. (2017b), droplet penetration in the sugarcane canopy will be enhanced.

Experimental results and discussion

Results of droplet deposition

The results of the droplet deposition amount are shown in Table 7.

TABLE 7. Results of the droplet deposition amount.

Serial number	Droplet deposition amount (μl/cm²)							
	Treatment 1		Treatment 2		Treatment 3		Treatment 4	
	Upper	Lower	Upper	Lower	Upper	Lower	Upper	Lower
1	0.0551	0.0020	0.0132	0.0045	0.0072	0.0244	0.0076	0.0046
2	0.0309	0.0052	0.0273	0.0282	0.0190	0.0488	0.0042	0.0003
3	0.0783	0.0006	0.0448	0.0415	0.2587	0.1229	0.0087	0.0042
4	0.0131	0.0014	0.2458	0.0460	0.2761	0.0505	0.0110	0.0129
5	0.4839	0.1031	0.8432	0.3887	0.7157	0.3049	0.0514	0.0310
6	0.1402	0.0453	1.1764	0.2214	0.9818	0.3491	0.0165	0.0137
7	0.5301	0.2351	0.9456	0.2533	0.0583	0.0468	0.0211	0.0080
8	0.0520	0.0358	0.2659	0.0321	0.0964	0.0309	0.2560	0.1244
9	0.0242	0.0148	0.4403	0.0097	0.0579	0.0316	0.0857	0.0423
10	0.0459	0.0359	0.1215	0.0293	0.0314	0.0229	0.0235	0.0194
11	0.0650	0.0538	0.0808	0.0479	0.0380	0.0236	0.0213	0.0049
12	0.0613	0.0591	0.0137	0.0275	0.0063	0.0199	0.0098	0.0213
13	0.0038	0.0018	0.0582	0.0123	0.0000	0.0010	0.0196	0.0137
14	0.0436	0.0032	0.0063	0.0067	0.0004	0.0029	0.0185	0.0082
15	0.0057	0.0001	0.0311	0.0015	0.0001	0.0041	0.0111	0.0050
16	0.0013	0.0003	0.0132	0.0006	0.0008	0.0086	0.0096	0.0003
17	0.0002	0.0001	0.0090	0.0001	0.0002	0.0005	0.0014	0.0026

Influences of the initial droplet velocities on droplet penetration in sugarcane protection

When the UAV carried out the agricultural spraying operation, the effective point was judged at the time when the droplet coverage density reached at least 15 droplets/cm² (Chen et al., 2017c). To characterize droplet penetration, the coefficient of variation (CV) of the droplet deposition amount in the upper and lower layers of each sampling rod was used to measure droplet penetration. The smaller the CV is, the better the droplet penetration.

Although the cone nozzle and the centrifugal nozzle have different initial vertical velocities, there is no significant difference in their penetration in the effective range (Table 8). The initial vertical velocity of the droplet does not advance the optimum penetration, which is consistent with the theoretical analysis (Table 9).

TABLE 8. Coefficients of variation of the droplet amount.

Treatment	Serial number of effective points	Coefficient of variation (%)	Mean coefficients of variation (%)	Treatment	Serial number of effective points	Coefficient of variation (%)	Mean coefficients of variation (%)
1	5	91.74	39.00	2	4	36.02	43.80
	6	72.35			5	9.26	
	7	54.52			6	84.38	
	8	26.09			7	61.72	
	9	34.09			8	47.54	
	10	17.29			9	85.01	
	11	13.33			10	14.22	
	12	2.58			11	12.27	
3	3	50.33	50.80	4			44.39
	4	97.69			5	35.01	
	5	56.92			6	13.11	
	6	67.23			7	63.66	
	7	15.47			8	48.92	
	8	72.77			9	47.95	
	9	41.56			10	13.52	
	10	22.14			11	88.52	
	11	33.06					

TABLE 9. Relative error of theoretical and experimental results.

Nozzle type	Theoretical results			Experiment results		
	Initial vertical velocity	Final vertical velocity	Relative error (%)	Initial vertical velocity	Droplet penetration	Relative error (%)
Centrifugal	0	2.44006	0	0	43.80	1.34
Cone	12	2.44006		12	44.39	

Influences of UAV flying heights on droplet penetration

The coefficients of variation of the droplet amounts with flying heights of 5.5 m, 6.0 m and 6.5 m are 39.00%, 43.80% and 50.80%, respectively (Table 8); therefore, it can be concluded that when the flying height decreases, droplet penetration improves (Figure 7).
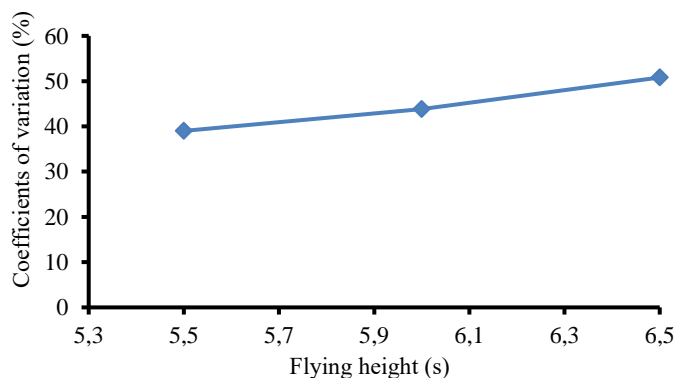

FIGURE 7. Effect of flying height on droplet penetration.

Qin (2017) showed that the downwash flow velocity near the crop canopy increases with decreasing UAV flying height. According to the calculation results in this paper, the vertical velocity of droplets will also increase. Therefore, the following conclusion can be drawn: an increase in the vertical velocity of droplets will improve droplet penetration, which is complementary to the research results of Chen et al. (2017b).

The amount of droplets deposited at the lower collection point can be greater than that at the upper collection point (Table 7). This situation occurs because the sugarcane plant may tilt under the action of rotor downwash flow, disturbing the leaves. A similar situation was reported by Chen et al. (2017d).

The penetration of droplets is not only related to the final droplet velocity but also affected by the plant height and canopy leaf area index (Sun & Liu, 2019). In addition, the droplet horizontal velocity has an important influence on the effective spray width and the deposition uniformity, so the flying height of the UAV should not be too low. In sugarcane protection using the TY-800 single-rotor UAV, the flying height should not be lower than 5.5 m to ensure that the sugarcane canopy does not shake violently.

Drag force is a decisive factor in droplet movement in the airflow field, and the properties of chemical pesticides barely influence droplet trajectory (Sun, 2018). Although the density and other physical properties of chemical pesticides are not the same as those of water, the research results of this paper can provide guidance for sugarcane plant protection.

CONCLUSIONS

When a droplet moves in the downwash flow field of a single-rotor UAV, the final vertical velocity of the droplet is positively related to the droplet diameter. The major factor affecting the droplet velocity is the downwash flow field of the UAV. There is no significant correlation between the final vertical droplet velocity and the initial droplet vertical velocity.

In the process of droplet transportation, the droplet velocity quickly approaches the downwash flow velocity. The droplet acceleration increases when the droplet diameter decreases and when the difference between the downwash flow velocity and the droplet velocity increases.

REFERENCES

Ahmed M, Youssef MS (2014) Influence of spinning cup and disk atomizer configurations on droplet size and velocity characteristics. Chemical Engineering Science 107(14):149-157.

An JL, Xiang WL, Han ZW, Xiao KT, Wang ZF, Wang XH, Wu JB, Yan PZ, Li J, Chen Y, Li J, Li Y (2013) Validation of the Institute of Atmospheric Physics emergency response model with the meteorological towers measurements and SF6 diffusion and pool fire experiments. Atmospheric Environment 81: 60-67.

Canata TF, José PM, Sousa RVD (2019) A measurement system based on lidar technology to characterize the canopy of sugarcane plants. Engenharia Agricola 39(2): 240-247.

Chen SD, Lan YB, Zhou ZY, Liao J, Zhu QY (2017a) Effects of spraying parameters of small plant protection UAV on droplets deposition distribution in citrus canopy. Journal of South China Agricultural University 38(5): 97-102.

Chen SD, Lan YB, Bradley KF, Li JY, Liu AM, Mao YD (2017b) Effect of wind field below rotor on distribution of aerial spraying droplet deposition by using multi-rotor UAV. Journal of agricultural machinery 48(08):105-113.

Chen SD, Lan YB, Li JY, Xu XJ, Wang ZG, Peng B (2017c) Evaluation and test of effective spraying on plant protection UAV. Transactions of the Chinese Society of Agricultural Engineering 33(7): 82-90.

Chen SD, Lan YB, Li JY, Zhou ZY, Liu AM, Xu XJ (2017d) Comparison of the pesticide effects of aerial and artificial spray applications for rice. Journal of South China Agricultural University 38(4): 103-109.

David D, Boon S, Silins U (2014) Watershed-scale controls on snow accumulation in a small montane watershed, southwestern Alberta, Canada. Hydrological Processes 28(3): 1294-1306.

Feng XY, Shen LB, Wang WZ, Wang JG, Cao ZY, Zhang SZ (2019) Reverse transcription recombinase polymerase amplification assay for the detection of Sugarcane streak mosaicvirus in sugarcane. Sugar Tech 21(4): 645–652.

Fritz BK, Hoffmann WC, Lan Y (2009) Evaluation of the EPA Drift Reduction Technology (DRT) Low-Speed Wind Tunnel Protocol. Journal of ASTM International 6(4):183-191.

Gao DW, Zhao C (2020) The shape and ending velocity of raindrops falling. Physics and Engineering 29(06): 65-70.

He XK (2004) Improving severe draggling actuality of plant protection machinery and its application techniques. Transactions of the Chinese Society of Agricultural Engineering 20(1):13-15.

Lee K, Han Y, Ha JI (2014) Minimum Copper Loss Control of a Single-Phase Grid-Connected Wound rotor machine over full speed range. Energy Conversion Congress and Exposition (ECCE), IEEE, 2719-2726.

Li YR, Yang LT (2009) New Developments in Sugarcane Industry and Technologies in China since 1990s. Southwest China Journal of Agricultural Science 22(5):1469-1476.

Pan XH, Huang CH, Xin DY (2009) Dominant natural enemies and biological control of sugarcane. Guangxi Agricultural Science 40(1):49-52.

Qin WC, Qiu BJ, Xue XY, Chen C, Xu ZF, Zhou QQ (2016) Droplet deposition and control effect of insecticides sprayed with an unmanned aerial vehicle against plant hoppers. Crop Protection 85: 79-88.

Qin WC (2017) Research on spraying parameters optimization for single rotor plant protection UAV. PhD Thesis, Jiangsu University, College of Engineering.

Santos, NBD (2019). Economic analysis of different hydraulic sprayers used in sugarcane (saccharum spp.). Engenharia Agricola 39(2): 225-233.

Song JL, Qi LJ, Sun XH, Wang J, Liu Q (2007) Study on Flying time and distributing characteristic of droplet from Sprayer. Journal of Agricultural Machinery 38(04): 54-57.

Stevanato P, Chiodi C, Broccanello C, Concheri G, Biancardi E, Pavli O, Skaracis G (2019) Sustainability of the Sugar Beet Crop. Sugar Tech 21(5): 703–716.

Sun CD, Liu CD (2019) Construction and application of droplet canopy penetration model for air-assisted spraying pattern. Transactions of the Chinese Society of Agricultural Engineering 35(15): 25-32.

Sun T (2018) Research on multiple factors mechanism of pesticide spray droplet movement in the air. Dalian University of Technology: 31-39.

Wei XH, Shao J, Xie LG, Lu XL (2016) Design and Experiment of Air-assisted Cotton Boom Sprayer with Separating Row and Spraying in Inside and Upper Canopy. Journal of agricultural machinery 47(1): 101-107.

Yang FB, Ma DW, Zhu ZH, Le GG (2013) Pneumatic catapult performance research based on the true thermodynamic process analysis. Journal of mechanical engineering 49(24): 167-174.

Yang ZL, Ge LZ, Qi LJ, Cheng YF, Wu YL (2018) Influence of UAV Rotor Down-wash Airflow on Spray Width. Journal of agricultural machinery 49(1): 116-122.

Yuan HZ, Wang GB (2015) Effects of droplet size and deposition density on field efficacy of pesticides. Plant Protection 41(6): 9-16.

Zhang XQ, Liang YJ, Qin ZQ, Li DW, Wei CY, Wei JJ, Li YR, Song XP (2019) Application of multi-rotor unmanned aerial vehicle application in management of stem borer (lepidoptera) in sugarcane. Sugar Tech 21(5): 847-852.

Zhou DG, Wang CF, Li Z, Chen Y, Gao SW, Guo JL, Lu WY, Su YC, Xu LP, Que YX (2016) Detection of Bar transgenic sugarcane with a rapid and visual loop-mediated isothermal amplification assay. Frontiers in Plant Science (7): 279–289.

Zhou QQ, Xue XY, Yang FB, Qin WC (2017) Trajectory and deposition distribution features of centrifugal atomization nozzle droplet. Journal of Jiangsu University (Natural Science Edition) 38(01): 18-23.

Zhu Y, Cheng M, Hua W, Zhang BF (2013) Sensorless Control Strategy of Electrical Variable Transmission Machines for Wind Energy Conversion Systems. IEEE Transactions on Magnetics 49(7): 3383-3386.